Manipulation of optical coherence of quantum-well excitons by transverse magnetic field

I. A. Solovev,[1,*] I. I. Yanibekov,[1] I. A. Babenko,[2] B. V. Stroganov,[1] S. A. Eliseev,[1] V. A. Lovcjus,[1] Yu. P. Efimov,[1] S. V. Poltavtsev,[2] Yu. V. Kapitonov,[1] and I. A. Yugova[2]

[1]*St. Petersburg State University, 198504 St. Petersburg, Russia*

[2]*Spin Optics Laboratory, St. Petersburg State University, 198504 St. Petersburg, Russia*

(Received 29 April 2022; revised 23 August 2022; accepted 25 August 2022; published 2 September 2022)

We have studied experimentally spin-dependent photon echoes from excitons in an InGaAs/GaAs quantum well subject to a transverse magnetic field (Voigt geometry). Larmor precession of the spins of the electron and heavy hole in an exciton leads to a periodic transfer of coherence between bright and dark exciton states. The increase in dephasing time due to the transition to the dark states could be useful for coherent control development. A comprehensive analysis shows a good agreement between a four-wave mixing experiment and the predictions of a theoretical treatment based on a five-level exciton model comprising a ground state and two pairs of bright and dark states. The extracted optical dephasing time of bright and dark excitons is equal to 30 and 130 ps, respectively. Exploiting the photon echo reveals evidence of electron Larmor precession with in-plane g factor $|g_{e,\perp}| = 0.44 \pm 0.05$ and heavy hole precession as well. The precession frequency of the latter depends nonlinearly on the applied magnetic field, and the corresponding g factor reaches a value of $|g_{h,\perp}| \approx 0.3$ at $B = 6$ T. Estimates for the heavy hole g-factor spreading as well as the isotropic exchange interaction constant are provided.

DOI: 10.1103/PhysRevB.106.115401

I. INTRODUCTION

Protocols based on the photon echo (PE) in the presence of a transverse magnetic field could be used to store the optical coherence in elementary excitations of semiconductor heterostructures and to recall it on demand. The initial step in all of these protocols is the optical coherence transfer between states with different total spin projections by the precession in the magnetic field. To carry out this operation, the system should satisfy the condition $T_2 > 2\pi/\Omega$, where T_2 is the optical dephasing time of the initial state and Ω is the angular precession frequency. For moderate magnetic fields ($\approx$1 T) the suitable systems in low-dimensional heterostructures are charged exciton complexes, such as trions [1,2] or donor-bound excitons [3], which exhibit long T_2 and reasonably high g factors. However, the use of neutral excitons for these purposes has not yet been successful due to short dephasing times [4] or the absence of oscillations in a magnetic field.

In this paper, we propose excitons as elementary excitations suitable for optical coherence manipulation with spin state control. Here and below, by optical coherence we mean the preservation of phase relations between the vacuum ground state and the excited state of the semiconductor. Spin coherence means the conservation of phase between different spin states of the exciton. We show that in high-quality InGaAs/GaAs quantum wells (QWs) with low indium content [5] the T_2 of excitons could be at least as long as 30 ps, which allows us to observe several periods of magnetic-field-induced precession in a spontaneous two-pulse PE experiment.

The fundamental difference between excitons and their charged complexes is the inaccessibility by light of one of the states involved in the precession, the so-called dark exciton state. In the case of GaAs-based nanostructures, such states are spin-forbidden excitons with total spin projections $S_z = \pm 2$, and the quantization z axis usually coincides with the growth axis of the structure. Optical incoherent emission from dark exciton states was observed in transition metal dichalcogenide monolayers by application of a transverse magnetic field of several tens of teslas [6,7] and by the near-field coupling to surface plasmon polaritons [8]. Brightening of dark exciton states in QWs [9], quantum dots (QDs) [10], and carbon nanotubes [11] was also reported. Coherent precession [12] as well as deterministic writing and control [13] of dark exciton spin via biexcitonic excitation without magnetic field was demonstrated in a single-QD system. In four-wave mixing (FWM) experiments, population transfer between bright and dark states was observed as a sequence of spin flips in GaAs/AlGaAs QWs [14] and in CdSe/CdS colloidal QDs [15]. Several studies have been carried out on the effects of a magnetic field on the exciton coherent dynamics on the femtosecond scale [16,17].

The PE protocol involving dark excitonic states promises additional possibilities for coherence storage and control. A special theoretical treatment was developed to describe these experiments [18]. Using this approach, in this paper we successfully untangle the temporal behavior of the spontaneous PE signal in different polarization geometries and transverse magnetic fields. Dephasing times of bright and dark exciton states were determined, as well as electron and hole g factors, and the roles of the exchange interaction and g-factor spreading were estimated. The PE protocol is the only method that is able to access all of these material parameters separately with sub-meV spectral resolution utilizing picosecond laser pulses.

*i.a.soloviev@spbu.ru

II. EXPERIMENTAL DETAILS

The system under study is a high-quality single QW. Sample P551 was grown by molecular beam epitaxy on a (100)-oriented GaAs wafer with rotation during growth. A 1000-nm-thick GaAs buffer layer was grown followed by the InGaAs QW with a thickness of 3 nm and indium concentration of 3–4% which was capped by a 170-nm-thick GaAs layer.

For optical characterization the sample was mounted in closed-cycle helium cryostats and kept at 10 K during reflection and at 4 K during photoluminescence (PL) studies. The laser excitation spot size on the sample surface was 50 × 50 μm in PL and 150 × 50 μm in reflectivity measurements. We exploited reflection spectroscopy in the Brewster geometry, which allows us to suppress the nonresonant background reflection from the sample surface. Following the approach of Refs. [5,19], in the case of low inhomogeneous broadening the observed resonance in the reflectance spectrum could be fit by a Lorentzian curve:

$$R(\omega) = \frac{\Gamma_0^2 \cos^2\varphi}{(\omega-\omega_0)^2 + (\Gamma_0\cos\varphi + \Gamma_{\rm NR})^2}, \qquad (1)$$

where Γ_0 and $\Gamma_{\rm NR}$ are the radiative and nonradiative decay rates of excitons, respectively, ω is the angular frequency of light, ω_0 is the exciton resonance angular frequency, and φ ($\approx$16°) is the angle of light incidence onto the QW layer. Measurement of both the amplitude of the peak $R(\omega_0) = \Gamma_0^2\cos^2\varphi/(\Gamma_0\cos\varphi + \Gamma_{\rm NR})^2$ and its half-width at half maximum (HWHM) $\Gamma = \Gamma_0\cos\varphi + \Gamma_{\rm NR}$ lets us obtain Γ_0 and $\Gamma_{\rm NR}$.

In photoluminescence (PL) measurements the circularly polarized excitation was tuned to the bulk GaAs exciton resonance $E = 1.515$ eV. The degree of circular polarization (DCP) of the PL signal was calculated in the following way: DCP $= \frac{I^+ - I^-}{I^+ + I^-}$, where I^+ (I^-) is the PL intensity at co-circularly-polarized (cross-circularly-polarized) excitation and detection. In order to investigate the coherent dynamics of excitons, we exploited the time-resolved degenerate FWM and two-pulse (spontaneous) PE techniques. The sample was kept at 1.5 K in liquid helium in a variable-temperature inset of a closed-cycle helium cryostat (Cryogenic) with a superconducting magnet being able to apply the transverse magnetic field up to 6 T. The sample was excited by a sequence of two linearly polarized laser pulses with a duration of 3 ps generated by a Spectra-Physics Tsunami Ti:sapphire laser. The sample excitation was carried out in a geometry close to normal with wave vectors $\vec{k}_1$ and $\vec{k}_2$ of the first and second laser pulses, respectively [see Fig. 1(a)]. The excitation spot diameter was 200 μm. The coherent FWM signal with $\vec{k}_{\rm FWM} = 2\vec{k}_2 - \vec{k}_1$ is collected in the reflection geometry. The cross correlation between the FWM signal and the reference laser pulse is detected by a balanced photoreceiver. Optical delay lines are used to tune the arrival times of the second exciting and the reference pulses relative to the first exciting pulse, denoted as τ and $\tau_{\rm Ref}$, respectively.

The polarization configuration of the PE experiment is denoted hereinafter as $XY \rightarrow Z$, where X and Y are polarizations of the first and second exciting pulses and Z is the reference pulse (detection) polarization. The transverse magnetic field lying in the QW plane (Voigt geometry) sets the direction of the main polarizations: The horizontal (H) one is parallel to the field, and the vertical (V) polarization is perpendicular to it [Fig. 1(a)].

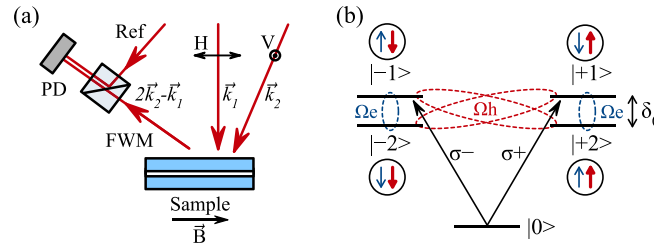

FIG. 1. (a) Sketch of FWM experimental setup. PD, photodetector; Ref, reference pulse. (b) Schematic representation of exciton energy states and interaction of the exciton with light in a transverse magnetic field. Solid black arrows correspond to circularly polarized optical transition, while dashed ellipses represent Larmor precession of electron (blue) and heavy hole (red) spins

Optical heterodyne detection was implemented. The first and reference pulses are frequency shifted by dual acousto-optical modulators by $f_1 = -81$ MHz and $f_2 = +80$ MHz, respectively, so that cross correlation between the FWM and the reference pulse is modulated at $|f_1 + f_2| = 1$ MHz. Additionally, the first pulse is mechanically chopped at $f = 1$ kHz for the second locked-in detection. Finally, we detect a background-free signal proportional to the absolute value of the FWM amplitude.

We applied the recently developed PE polarimetry method to confirm the excitonic nature of the studied resonance [20,21]. Since excitons and trions have different PE responses to the polarization configuration of excitation, we are able to use this feature for determination of the exciton transition. Particularly, when exciting pulses are linearly polarized and their polarization planes are rotated relative to each other by the angle φ, the PE from excitons is also linearly polarized and collinear with the second pulse with the amplitude $\propto \cos(\varphi)$ [21].

Femtosecond laser excitation with a spectral width of about 20 meV was previously used to study the FWM and PE from QWs [16,22–25]. Such spectrally wide excitation generally induces simultaneous transitions between the ground state and several exciton states, exciton complexes, and biexcitons, which leads to the observation of complex temporal beats in the time-resolved PE signal even without a magnetic field. In this paper, using picosecond laser pulses with a typical spectrum width of 1 meV, we succeeded in selectively addressing the exciton transition and eliminating many-body effects. Thus biexciton states could be excluded from theoretical consideration.

III. EXPERIMENTAL RESULTS AND DISCUSSION

A. Linear spectroscopy of an isolated exciton in a QW

A typical reflectivity spectrum of the QW sample at low temperature plotted in terms of energy units on the x axis is shown in Fig. 2(a). It is dominated by the resonance of a heavy hole exciton in the QW (X) with a spectral position

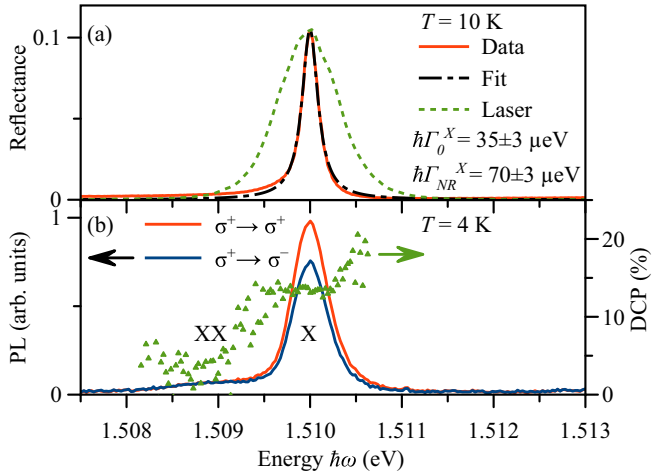

FIG. 2. (a) Typical reflectivity spectrum measured in the Brewster geometry (solid curve), approximation of reflection spectrum by a Lorentzian curve (long-and-short-dashed curve), and excitation laser spectrum (short-dashed curve) used for the FWM experiment. (b) PL spectra for σ^+-polarized excitation and copolarized (red) and cross-polarized (blue) detection and DCP spectrum (triangles).

$E_X = 1.510$ eV, amplitude of 0.1, and HWHM of 105 μeV. From fitting we obtained values of the radiative width $\hbar\Gamma_0^X = 35 \pm 3$ μeV and the nonradiative broadening $\hbar\Gamma_{\rm NR}^X = 70 \pm 3$ μeV. The nonradiative broadening is only twice larger than the radiative width, which indicates the high quality of the sample and efficient optical coherence transfer between light and excitons [5].

PL spectra at $T = 4$ K are shown in Fig. 2(b). The red and blue curves correspond to co-circularly-polarized and cross-circularly-polarized detection, respectively. The exciton peak in PL spectra (X) shows almost no Stokes shift in comparison to the reflectivity spectrum. At high excitation intensity, an additional peak emerges at $E_{XX} = 1.509$ eV which we identify as a heavy hole biexciton (XX) emission. DCP measurement [Fig. 2(b), triangles] shows that exciton PL retains the excitation polarization while biexciton emission is almost unpolarized. Such behavior is typical for an exciton-biexciton system [26]. The extracted energy splitting $E_{b(XX)} = 1.1 \pm 0.2$ meV is generally consistent with the biexciton binding energy reported for GaAs/AlGaAs and InGaAs/GaAs QWs [22,26,27]. Thus the usage of spectrally narrow picosecond excitation allowed us to isolate the exciton resonance and to be sure that no other states are excited by a laser pulse. The following studies of the FWM were performed with the laser tuned to the X resonance.

B. PE from excitons

1. Zero magnetic field

The time-resolved FWM signal measured in the absence of a magnetic field in the HH → H geometry is shown in Fig. 3(a) for different time delays between exciting pulses τ. The FWM response has the form of a peak centered at time $\tau_{\rm Ref} = 2\tau$, which is a clear manifestation of the conventional two-pulse PE from an inhomogeneously broadened exciton ensemble [28–30]. The waveform tends to a Gaussian curve

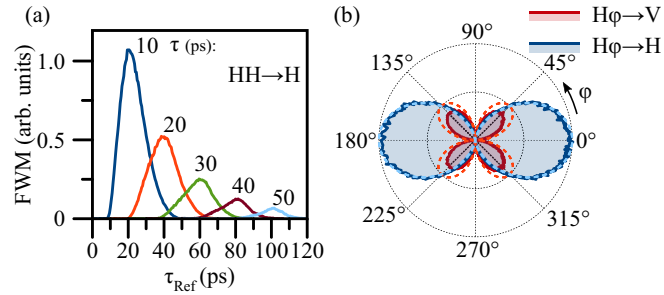

FIG. 3. (a) Temporal profiles of FWM signal from excitons in a QW measured at different time delays τ. (b) Experimental (solid curve) and theoretical (dashed curve) [21] dependencies of PE amplitude at $\tau = 15$ ps on angle φ between first and second excitation pulse polarizations with the H-polarized first pulse and H- (blue) and V-polarized (red) detection.

with 20 ps temporal width as τ increases. It should be noted that the presented signal is the cross correlation of the FWM and a 3-ps reference pulse. Nevertheless, the large PE temporal width allows us to assume that the presented data reflect the near-true profile of the PE and the effect of broadening due to convolution of the PE with the reference pulse during registration can be neglected. Such a long duration of the PE corresponds to a comparably low inhomogeneity of the exciton ensemble with a spectral width of 92 μeV. The PE peak amplitude decays exponentially with characteristic optical dephasing time $T_2 = 30$ ps. Furthermore, we will focus only on this maximum of the PE amplitude, i.e., the cross-correlation signal detected at $\tau_{\rm Ref} = 2\tau$. The polarimetric measurements presented in Fig. 3(b) show the PE amplitude dependence on φ when detection polarization is parallel and perpendicular to polarization of the first pulse, correspondingly. The visually striking property of the excitonic PE is its polarization along the second-pulse polarization direction and the cosine dependence of the PE amplitude $\propto \cos(\varphi)$. Curve Hφ → H exhibits two equal maxima, while curve Hφ → V has four equal maxima, the amplitude of which is almost two times smaller than in the Hφ → H geometry as predicted theoretically [21] for an exciton level structure. The measurements coincide qualitatively with theoretical modeling and additionally prove that this is a pure neutral exciton system.

2. PE decay in a magnetic field

The key experiment is the measurement of PE amplitude as a function of τ, which we call PE decay. Figure 4 illustrates PE decays in HH → H and VV → V geometries with the application of the transverse magnetic field B. At zero B the signal decays exponentially in the same way for both geometries with dephasing time of bright excitons $T_2^b = 30$ ps as additionally shown in Fig. 5. Spectrally narrow picosecond excitation makes it possible to observe the pure excitonic signal without evidence of exciton-biexciton quantum beatings [25] and allows us to exclude the biexciton state from theoretical consideration.

The application of the transverse magnetic field B parallel to H polarization (Voigt geometry) changes the picture dramatically. The PE decay becomes oscillating for both

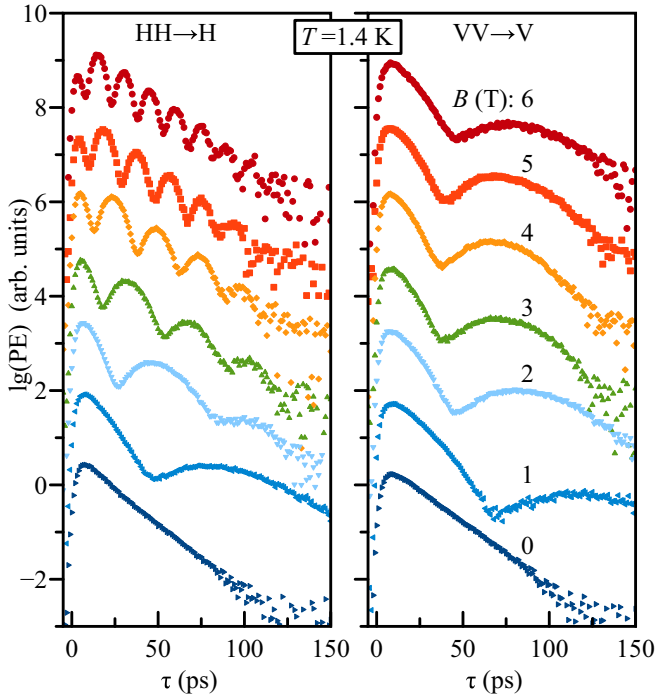

FIG. 4. PE decays from excitons in transverse magnetic field. The curves are offset vertically for clarity. Here, lg, is common logarithm.

geometries. In the HH → H configuration the oscillation frequency rises with increasing B, while in VV → V the curve weakly depends on field at $B \geqslant 2$ T. At high magnetic field the oscillation amplitude is damping with rising τ. An unexpected behavior is observed at $B = 1$ T in the HH → H geometry and magnetic fields from 1 to 6 T in VV → V. In these cases, instead of periodic oscillations, a nonperiodic regime is observed, in which the PE signal passes through a minimum only once and then slowly decays with time much longer than T_2^b. Thus the observed complex dependence of the PE signal on the τ, magnetic field, and polarization geometry requires the construction of a special theoretical model describing it.

3. Model and discussion

The spectral isolation of the exciton transition in the QW makes it possible to omit biexcitonic states and consider a more straightforward five-level model, shown in Fig. 1(b). It includes the ground state and four heavy hole exciton states: two optically active bright states with the projection of total angular momentum $S_z = \pm 1$ and two optically inactive dark ones with $S_z = \pm 2$. More details about the exciton fine structure are provided in the Appendix.

Let us clarify that oscillations in the PE decay are caused by the action of a magnetic field on excitons. The transverse magnetic field causes Larmor precession of electron and hole spins in the exciton (see the Appendix), which is schematically illustrated in Fig. 1(b) with dashed ellipses. As a result, it mixes bright and dark exciton states during the time of formation of the PE [1,2].

Such a PE experiment can be modeled analytically by the solution of the Lindblad equation for the density matrix in the rotating wave approximation considering infinitely short optical excitation; see the Appendix for details. It is important to take into account the dephasing rates of bright γ_b and dark γ_d excitonic states and isotropic exchange interaction δ_0 as well. The expression for the PE amplitude P in the case of collinear polarizations of the exciting pulses and detection takes the following form:

$$P(\alpha) \propto e^{-2\gamma\tau} \underbrace{|R_H \cos^2\alpha + R_V \sin^2\alpha|^2}_{R}, \tag{2}$$

where $\gamma = \frac{\gamma_b+\gamma_d}{2}$ is the average dephasing rate and α is the angle between the polarization plane of light and the magnetic field. The two components $R_{H,V}$ are defined in the following way:

$$R_{H,V} = \cos(\Omega_{H,V}\tau) + \frac{i\frac{\delta_0}{2\hbar} - \Delta\gamma}{\Omega_{H,V}} \sin(\Omega_{H,V}\tau), \tag{3}$$

where $\Omega_{H,V}$ is the effective Larmor precession angular frequency,

$$\Omega_{H,V} = \sqrt{\Omega_{0H,V}^2 + \left(\frac{\delta_0}{2\hbar} + i\Delta\gamma\right)^2}, \tag{4}$$

$$\Omega_{0H,V} = \frac{\omega_e \pm \omega_h}{2}, \quad \Delta\gamma = \frac{\gamma_b - \gamma_d}{2}. \tag{5}$$

Here, ω_e and ω_h are the electron and hole Larmor precession angular frequencies. P has the simplest form when $\alpha = 0°$ [HH → H geometry; see Fig. 1(a)] and $\alpha = 90°$ (VV → V) that determines the choice of these polarization configurations for measurements.

The derived expression (2) fits properly PE decays for the whole range of magnetic fields. We will discuss below the most significant features of the model in comparison to

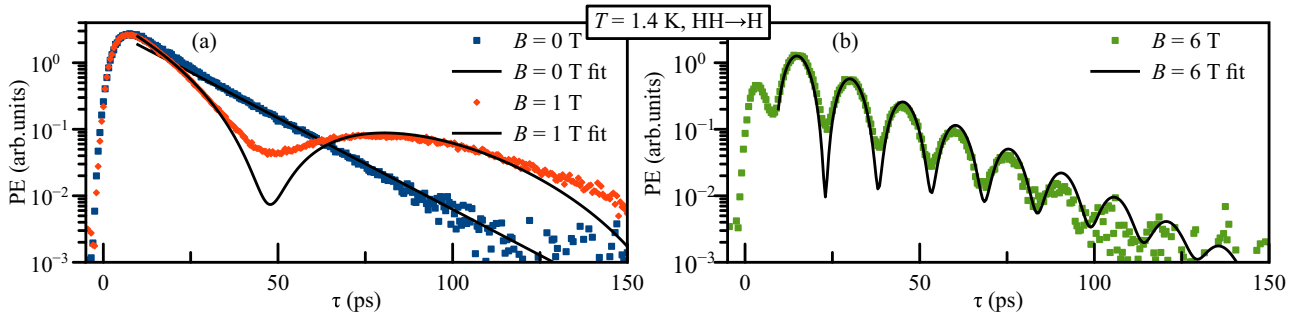

FIG. 5. PE decays from excitons (symbols) and their theoretical fits (solid curves) at $B = 0$ and 1 T (a) and $B = 6$ T (b).

the experimental data. To do this, we will refer to Fig. 5, where the most illustrative cases are shown.

At zero field B, expression (2) is reduced to monoexponential decay $P \propto e^{-2\gamma_b \tau}$ corresponding to the conventional case of a PE from a bright exciton ensemble as shown in Fig. 5(a). At $B > 0$ the oscillating term R induced by Larmor precession is superimposed on exponential decay. Shuffling the coherence between bright and dark excitons with different dephasing rates $\gamma_{b,d}$ leads to significant changes: Henceforth the precession frequency $\Omega_{H,V}$ depends also on the difference $\Delta\gamma$. The term R could be divided into oscillating and decaying terms that determine the PE temporal behavior. However, when the difference in rates is quite small compared with the Larmor frequency $\Delta\gamma \ll |\Omega_{0H,V}|$ and $\delta_0/\hbar \to 0$, the behavior is very close to the product of exponential decay and a single-frequency harmonic function. If $\gamma_b = \gamma_d$, expression (2) coincides with the result of the modeling considered in Ref. [20]:

$$P^{H,V} \propto e^{-2\gamma_b \tau}\left(\cos^2(\Omega_{H,V}\tau) + \frac{\delta_0^2}{4\hbar^2}\frac{\sin^2(\Omega_{H,V}\tau)}{\Omega_{H,V}^2}\right). \quad (6)$$

A similar situation with correction of decay time is realized at high fields $B \geqslant 3$ T in the HH $\to$ H geometry (Fig. 4). The most characteristic case of such behavior at $B = 6$ T and its theoretical fit are shown in Fig. 5(b). In other cases, the behavior is quite different, and the impact of $\Delta\gamma$ has to be considered.

We provided a detailed theoretical analysis of the spin-dependent PE from excitons in a QW in the case of different dephasing rates for bright and dark excitons and negligible exchange interaction in Ref. [18]. The main unexpected result is a transition to a nonperiodical regime when $\Delta\gamma \geqslant |\Omega_{0H,V}|$, manifesting itself as a single bounce in the PE decay curve separating segments with decay rates close to γ_b and γ_d. Transfer of coherence from fast-relaxing bright exciton states to long-lived dark ones is the origin of such nontrivial dynamics. Such a regime with nonharmonic decay is realized at moderate fields $B \leqslant 1$ T in the HH $\to$ H geometry [Fig. 5(a)] and almost at the whole available range of fields in the VV $\to$ V geometry (Fig. 4).

The basic model (6) from previous work [20] states that oscillating PE decay is always limited from above by monoexponential decay with a characteristic time of bright excitons. In contrast, we observe an increase in signal by almost an order of magnitude at $B = 1$ T and $\tau \approx 100$ ps as shown in Fig. 5(a). The advanced model [see Eq. (2)], which includes the impact of $\Delta\gamma$, describes such an effect as a manifestation of the coherent dynamics of long-lived dark excitons. From fitting we obtain dark exciton dephasing time $T_2^d = 130 \pm 30$ ps. Our recent measurements reveal that at lower magnetic field $B = 0.4$ T, T_2^d even exceeds 200 ps, which is around six times longer than T_2^b [18]. The main reason for such a difference in dephasing times must be the absence of a radiative channel of energy relaxation for spin-forbidden dark states, which limits phase relaxation. As a result, one could apply such a mixing of bright states with long-lived dark onesto increase the dephasing time of the system.

Under condition $\Omega_{0H} = \Omega_{0V}$, PE decays in collinear configurations should coincide; however, in Fig. 4 we clearly see

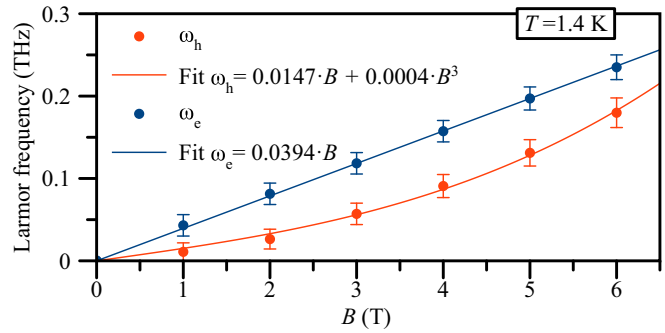

FIG. 6. Electron (blue) and heavy hole (red) Larmor precession angular frequencies extracted from PE decays as a function of magnetic field amplitude with corresponding linear and cubic approximations.

different behavior, revealing that both electron Larmor precession and heavy hole Larmor precession take place during the PE experiment under the action of the transverse magnetic field. Therefore it is worth measuring the PE decay in both the HH $\to$ H and VV $\to$ V geometries to get rich information about electron and heavy hole spin dynamics.

Frequencies ω_e and ω_h obtained from fitting of experimental data are depicted in Fig. 6 as a function of the applied transverse magnetic field. The electron Larmor frequency depends linearly on the magnetic field, which allows us to extract the in-plane electron g factor $|g_{e,\perp}| = 0.44 \pm 0.05$ from the fit with the equation $\omega_e = \frac{g_{e,\perp}\mu_B B}{\hbar}$. The obtained value of the g factor coincides with that for bulk GaAs [31–33] and is in line with values for thin InGaAs/GaAs QWs [34,35]. This indicates that the electron wave function is distributed mostly in GaAs barriers, which is expected due to the low percentage of indium in the QW layer and small QW thickness.

Along with electron spin oscillations we managed to observe heavy hole Larmor precession. Moreover, the frequency ω_h depends nonlinearly on the applied transverse magnetic field. The corresponding in-plane heavy hole g factor becomes comparable to the electron one at $B = 6$ T and reaches a maximum value of $|g_{h,\perp}| \approx 0.3$. The value of $g_{h,\perp}$ is usually assumed to be very small or even zero for simplicity (see the Appendix). However, there are several reports of nonzero $g_{h,\perp}$ where it was mainly determined by the Luttinger coefficient q [36] or both cubic anisotropy and other low-symmetry perturbations [37–39]. The obtained value of $|g_{h,\perp}|$ is within the range 0.15–0.6 of values measured in InGaAs/GaAs QDs where both strain and an admixture of light holes in a heavy hole state take place [40,41]. A dependence of the in-plane heavy hole g factor on the magnetic field in III–V structures was recently reported as a result of both the interface and magnetic-field-induced mixing of the heavy hole and light hole states [42]. In addition, the third-order perturbation theory also predicts a contribution to heavy hole splitting [43]. Experimental data are well approximated by a cubic function as shown in Fig. 6. However, the coefficient of the cubic term defined by heavy-hole–light-hole splitting is a thousand times less than the value we obtain from fitting. In our case, any of the above-mentioned contributions to $g_{h,\perp}$ are admissible, and we are not able to distinguish between different

mechanisms with the available data. Additional experiments as in Refs. [38,39] might be helpful for identification of individual contributions, and this is the subject of further work. It is worth noting that the advantage of the PE method is the observation of the sum and difference of Larmor frequencies of charge carriers, which, in contrast to other techniques, makes it possible to determine both frequencies with high accuracy even at low magnetic fields and in the case of a small difference between frequencies.

Our measurements provide only absolute values of g factors, and we see that both of them have the same sign. Relying on previous reports of a negative electron g factor in similar structures [34,35], it follows that the hole g factor is also negative in our description.

The zero of the PE signal is expected when there is no polarization in the optically accessible states ($\rho_{01} = \rho_{02} = 0$) at the arrival time of the second rephasing pulse τ. It is clear from Figs. 4 and 5 that oscillating decays do not reach zero value. At least two mechanisms lead to such behavior. The first one is the isotropic exchange interaction responsible for bright-dark splitting. The fitting of experimental data presented in Fig. 5 provides an estimate for the value of $\delta_0 \leqslant 10$ μeV. The second mechanism is attributed to inhomogeneous spreading of g factors, which is known to be as high as one-third of the g-factor modulus for heavy holes in InGaAs/GaAs quantum dots [44]. The inhomogeneity leads to smoothing of oscillations in the vicinity of PE zeros and to a decrease in the oscillation contrast at long time delay and high field as well. This spreading could be taken into account by convolution of the PE signal with the Gaussian distribution function of heavy hole g factors in the studied ensemble of excitons: $P_\Sigma \sim \int P e^{-\frac{(g_h - g_{h0})^2}{2\Delta g_h^2}} dg_h$, where P_Σ is the integrated PE polarization, P is the PE polarization from the subensemble with g_h, g_{h0} is the mean g factor, and Δg_h is the g-factor spreading. Figure 5 shows the best fit for $\frac{\Delta g_h}{g_h} = 0.03$. It should be noted that both the exchange interaction and g-factor spreading manifest in experiment similarly in the case of their small values, so we can obtain only upper estimates for these parameters.

IV. CONCLUSIONS

In this paper, we have shown the possibility of manipulating the optical coherence of excitons in InGaAs/GaAs single QWs using a transverse magnetic field, thus placing neutral excitons on par with trions and donor-localized excitons as candidates for creating optical devices based on PE protocols. The presence of optically inaccessible dark excitonic states leads to the appearance of modes of the PE kinetics in a magnetic field that are unattainable in charged exciton complexes. To explain the full temporal, magnetic field, and polarization dependence of the two-pulse PE signal from excitons, we constructed a theoretical model that takes into account the difference between the dephasing times of bright and dark excitons, the Larmor precession frequency of charge carriers, the isotropic exchange interaction, and the distribution of g factors. Only a complete consideration of all these processes made it possible to obtain a satisfactory description of the experimental results. The nonlinear field dependence of the heavy hole g factor was revealed owing to the high accuracy of the spin-dependent PE method in the range of small magnetic fields.

ACKNOWLEDGMENTS

This work was supported by Russian Science Foundation Grant No. 22-22-00439 [45]. This work was carried out on the equipment of the SPbU Resource Center "Nanophotonics."

APPENDIX: ADDITIONAL THEORETICAL ASPECTS

1. Exciton Larmor precession

In the classical picture an electron traveling in a circular orbit around the nucleus has a magnetic dipole moment $\vec{m}$ proportional to an electron angular momentum $\vec{L}$ through the gyromagnetic ratio. The external magnetic field $\vec{B}$ induces rotation of $\vec{m}$ about the vector $\vec{B}$ at the Larmor frequency. Considering quantum objects, in addition to $\vec{L}$ there is an intrinsic angular momentum spin $\vec{S}$ [46], and the $\vec{m}$ of charged quasiparticles is related to total angular momentum (also called spin) $\vec{J} = \vec{L} + \vec{S}$ through the g factor [32,44,47]. In the trivial case of a single electron with initially degenerate states characterized by spin projection on the fixed axis $s_z = \pm 1/2$, applying transverse magnetic field $\vec{B} = (B_x, 0, 0)$ leads to oscillation of the average value of $\langle s_z \rangle$ between $+1/2$ and $-1/2$ at the Larmor frequency determined by Zeeman splitting of electron states $\Delta E = g\mu_B B_x$ similar to the classical case.

The lowest exciton state in GaAs-based nanostructures is formed of an electron in the conduction band with spin $j^e = s^e = 1/2$ ($l^e = 0$, $s^e = 1/2$) and a heavy hole in the valence band with $j^{hh} = 3/2$ ($l^{hh} = 1$, $s^{hh} = 1/2$) [32,47–49]. In Voigt geometry, oscillation of the average value of the electron spin projection on the growth direction (z) $s_z^e = \pm 1/2$ leads to mixing of the optically accessible bright exciton state $J_z = +1$ ($J_z = -1$) with the optically inaccessible dark state $J_z = +2$ ($J_z = -2$), while oscillation of the heavy hole spin projection $j_z^{hh} = \pm 3/2$ mixes state $J_z = +1$ ($J_z = -1$) with state $J_z = -2$ ($J_z = +2$) [48,50,51].

The heavy hole g factor is known to be strongly anisotropic in confined GaAs-based nanostructures [37] since lowering of dimensionality leads to splitting of heavy and light holes with corresponding spin projections $\pm 3/2$ and $\pm 1/2$. As a result, heavy hole Zeeman splitting in a transverse magnetic field is zero because of the zero matrix of operator $J_x = J_y = 0$ [34,35,51]. Non-Zeeman interaction of hole spins with magnetic field which is admissible by the symmetry of the Luttinger Hamiltonian is described by cubic terms J_x^3, J_y^3 with Luttinger parameter q [37,43]. The latter is usually assumed to be very small or even zero for simplicity.

2. Spin-dependent PE from excitons

In order to describe optical coherent dynamics of excitons in a QW subject to a transverse magnetic field, we follow the theoretical approach used for the description of spin-dependent photon echo from trions [1,38]. We consider a five-level exciton system: the ground state of the crystal with spin projection onto the growth direction (z) $S_z = 0$, two optically bright exciton states with $S_z = \pm 1$, and two

optically dark ones with $S_z = \pm 2$. The energy scheme of the unperturbed system is illustrated in Fig. 1(b). At zero magnetic field the exchange interaction between electron and hole spins determined by the spin mutual orientation causes splitting of exciton states. The energy space between bright and dark exciton doublets is defined by the isotropic exchange interaction constant δ_0. Anisotropic exchange interaction causes additional splitting of these doublets. We set anisotropic exchange interaction constants $\delta_{1,2}$ to zero for simplicity due to their smallness. The detailed analysis of the exciton fine structure was done for GaAs-based QWs [51] and QDs [48].

The temporal evolution of the exciton ensemble is described by the Lindblad equation for the exciton density matrix:

$$\dot{\rho} = -\frac{i}{\hbar}[\hat{H}, \rho] + \Gamma, \tag{A1}$$

where $\hat{H}$ is the Hamiltonian of the exciton system and Γ is the relaxation term introduced phenomenologically which contains phase relaxation terms only.

The Hamiltonian includes three contributions which characterize the unperturbed exciton system, interaction of light with bright excitons, and action of a transverse magnetic field. The total Hamiltonian has the following form in basis $S_z = \{0; +1; -1; +2; -2\}$:

$$\hat{H} = \frac{\hbar}{2}\begin{pmatrix} 0 & f_+^* e^{i\omega t} & f_-^* e^{i\omega t}; & 0 & 0 \\ f_+ e^{-i\omega t} & 2\omega_0 + \delta_0/\hbar & 0 & \omega_e & \omega_h \\ f_- e^{-i\omega t} & 0 & 2\omega_0 + \delta_0/\hbar & \omega_h & \omega_e \\ 0 & \omega_e & \omega_h & 2\omega_0 - \delta_0/\hbar & 0 \\ 0 & \omega_h & \omega_e & 0 & 2\omega_0 - \delta_0/\hbar \end{pmatrix}. \tag{A2}$$

Here, ω_0 is the exciton resonance angular frequency, and ω is the angular frequency of exciting electromagnetic field. $f_\pm$ is proportional to the smooth envelope of the circularly polarized component $\sigma\pm$ of the excitation pulse and to the matrix element of the transition dipole moment between the vacuum and bright exciton states ± 1. The rotating wave approximation is used to get rid of fast-oscillating terms in $\hat{H}$ [52]. Macroscopic polarization in the form of a PE pulse is obtained by integration over the ensemble of excitons with inhomogeneously broadened resonant frequency ω_0.

Calculations can be significantly simplified by separating in time the action of the magnetic field and the interaction with light pulses. Such a procedure is suitable since at the considered magnetic field amplitudes the Larmor precession period is much longer than the pulse duration of about 3 ps and the Zeeman Hamiltonian may be omitted during the action of the laser pulses [1–3,20]. The resulting expression for the PE amplitude in collinear geometry is the following:

$$P \propto e^{-(\gamma_b+\gamma_d)\tau} \underbrace{(|R_1|^2 + |R_2|^2\cos^2(2\alpha) + 2\cos(2\alpha)\mathrm{Re}\{R_1 R_2^*\})}_{R}, \tag{A3}$$

$$R_{1,2} = \cos(\Omega_+\tau) \pm \cos(\Omega_-\tau) + \frac{i(\delta_0/\hbar + i(\gamma_b - \gamma_d))}{2}\left(\frac{\sin(\Omega_+\tau)}{\Omega_+} \pm \frac{\sin(\Omega_-\tau)}{\Omega_-}\right), \tag{A4}$$

$$\Omega_\pm = \frac{1}{2}\sqrt{(\delta_0/\hbar + i(\gamma_b - \gamma_d))^2 + (\omega_e \pm \omega_h)^2}. \tag{A5}$$

Equation (2) can be obtained from Eq. (A3) after some algebra.

[1] L. Langer, S. V. Poltavtsev, I. a. Yugova, D. R. Yakovlev, G. Karczewski, T. Wojtowicz, J. Kossut, I. a. Akimov, and M. Bayer, Magnetic-Field Control of Photon Echo from the Electron-Trion System in a CdTe Quantum Well: Shuffling Coherence between Optically Accessible and Inaccessible States, Phys. Rev. Lett. **109**, 157403 (2012).

[2] L. Langer, S. V. Poltavtsev, I. A. Yugova, M. Salewski, D. R. Yakovlev, G. Karczewski, T. Wojtowicz, I. A. Akimov, and M. Bayer, Access to long-term optical memories using photon echoes retrieved from semiconductor spins, Nat. Photonics **8**, 851 (2014).

[3] S. V. Poltavtsev, I. A. Yugova, I. A. Babenko, I. A. Akimov, D. R. Yakovlev, G. Karczewski, S. Chusnutdinow, T. Wojtowicz, and M. Bayer, Quantum beats in the polarization of the spin-dependent photon echo from donor-bound excitons in CdTe/(Cd,Mg)Te quantum wells, Phys. Rev. B **101**, 081409(R) (2020).

[4] I. A. Solovev, S. V. Poltavtsev, Y. V. Kapitonov, I. A. Akimov, S. Sadofev, J. Puls, D. R. Yakovlev, and M. Bayer, Coherent dynamics of localized excitons and trions in ZnO/(Zn,Mg)O quantum wells studied by photon echoes, Phys. Rev. B **97**, 245406 (2018).

[5] S. Poltavtsev, Y. Efimov, Y. Dolgikh, S. Eliseev, V. Petrov, and V. Ovsyankin, Extremely low inhomogeneous broadening of exciton lines in shallow (In,Ga)As/GaAs quantum wells, Solid State Commun. **199**, 47 (2014).

[6] Z. Lu, D. Rhodes, Z. Li, D. van Tuan, Y. Jiang, J. Ludwig, Z. Jiang, Z. Lian, S. F. Shi, J. Hone, H. Dery, and D. Smirnov, Magnetic field mixing and splitting of bright and dark excitons in monolayer $MoSe_2$, 2D Mater. **7**, 015017 (2020).

[7] X. X. Zhang, T. Cao, Z. Lu, Y. C. Lin, F. Zhang, Y. Wang, Z. Li, J. C. Hone, J. A. Robinson, D. Smirnov, S. G. Louie, and T. F. Heinz, Magnetic brightening and control of dark excitons in monolayer WSe_2, Nat. Nanotechnol. **12**, 883 (2017).

[8] Y. Zhou, G. Scuri, D. S. Wild, A. A. High, A. Dibos, L. A. Jauregui, C. Shu, K. De Greve, K. Pistunova, A. Y. Joe, T. Taniguchi, K. Watanabe, P. Kim, M. D. Lukin, and H. Park, Probing dark excitons in atomically thin semiconductors via near-field coupling to surface plasmon polaritons, Nat. Nanotechnol. **12**, 856 (2017).

[9] S. Glasberg, H. Shtrikman, I. Bar-Joseph, and P. C. Klipstein, Exciton exchange splitting in wide GaAs quantum wells, Phys. Rev. B **60**, R16295 (1999).

[10] M. Bayer, O. Stern, A. Kuther, and A. Forchel, Spectroscopic study of dark excitons in $In_xGa_{1-x}As$ self-assembled quantum dots by a magnetic-field-induced symmetry breaking, Phys. Rev. B **61**, 7273 (2000).

[11] S. Zaric, Optical signatures of the Aharonov-Bohm phase in single-walled carbon nanotubes, Science **304**, 1129 (2004).

[12] E. Poem, Y. Kodriano, C. Tradonsky, N. H. Lindner, B. D. Gerardot, P. M. Petroff, and D. Gershoni, Accessing the dark exciton with light, Nat. Phys. **6**, 993 (2010).

[13] I. Schwartz, E. R. Schmidgall, L. Gantz, D. Cogan, E. Bordo, Y. Don, M. Zielinski, and D. Gershoni, Deterministic Writing and Control of the Dark Exciton Spin Using Single Short Optical Pulses, Phys. Rev. X **5**, 011009 (2015).

[14] O. Ikeuchi, S. Adachi, H. Sasakura, and S. Muto, Observation of population transfer to dark exciton states by using spin-diffracted four-wave mixing, J. Appl. Phys. **93**, 9634 (2003).

[15] N. Accanto, F. Masia, I. Moreels, Z. Hens, W. Langbein, and P. Borri, Engineering the spin-flip limited exciton dephasing in colloidal CdSe/CdS quantum dots, ACS Nano **6**, 5227 (2012).

[16] U. Siegner, M.-A. Mycek, S. Glutsch, and D. S. Chemla, Quantum interference in the system of Lorentzian and Fano magnetoexciton resonances in GaAs, Phys. Rev. B **51**, 4953 (1995).

[17] S. T. Cundiff, R. Hellmann, M. Koch, G. Mackh, A. Waag, G. Landwehr, W. H. Knox, and E. O. Göbel, Excitonic dephasing in semimagnetic semiconductors, J. Opt. Soc. Am. B **13**, 1263 (1996).

[18] I. A. Solovev, I. I. Yanibekov, Y. P. Efimov, S. A. Eliseev, V. A. Lovcjus, I. A. Yugova, S. V. Poltavtsev, and Y. V. Kapitonov, Long-lived dark coherence brought to light by magnetic-field controlled photon echo, Phys. Rev. B **103**, 235312 (2021).

[19] E. Ivchenko, V. Kochereshko, P. Kop'ev, V. Kosobukin, I. Uraltsev, and D. Yakovlev, Exciton longitudinal-transverse splitting in GaAs/AlGaAs superlattices and multiple quantum wells, Solid State Commun. **70**, 529 (1989).

[20] I. Babenko, I. Yugova, S. Poltavtsev, M. Salewski, I. Akimov, M. Kamp, S. Höfling, D. Yakovlev, and M. Bayer, Studies of photon echo from exciton ensemble in (In,Ga)As quantum dots, in *VI International Conference "Modern Nanotechnologies and Nanophotonics for Science and Industry"9–13 November 2017, Suzdal, Russian Federation*, Journal of Physics: Conference Series Vol. 951 (Institute of Physics, London, 2018), p. 012029.

[21] S. V. Poltavtsev, Y. V. Kapitonov, I. A. Yugova, I. A. Akimov, D. R. Yakovlev, G. Karczewski, M. Wiater, T. Wojtowicz, and M. Bayer, Polarimetry of photon echo on charged and neutral excitons in semiconductor quantum wells, Sci. Rep. **9**, 5666 (2019).

[22] P. Borri, W. Langbein, J. M. Hvam, and F. Martelli, Binding energy and dephasing of biexcitons in $In_{0.18}Ga_{0.82}As$/GaAs single quantum wells, Phys. Rev. B **60**, 4505 (1999).

[23] M. Koch, D. Weber, J. Feldmann, E. O. Göbel, T. Meier, A. Schulze, P. Thomas, S. Schmitt-Rink, and K. Ploog, Subpicosecond photon-echo spectroscopy on GaAs/AlAs short-period superlattices, Phys. Rev. B **47**, 1532 (1993).

[24] J. Feldmann, T. Meier, G. Von Plessen, M. Koch, E. O. Göbel, P. Thomas, G. Bacher, C. Hartmann, H. Schweizer, W. Schäfer, and H. Nickel, Coherent Dynamics of Excitonic Wave Packets, Phys. Rev. Lett. **70**, 3027 (1993).

[25] M. Ikezawa, S. Nair, F. Suto, Y. Masumoto, C. Uchiyama, M. Aihara, and H. Ruda, Photon echo study of excitons and excitonic complexes in self-assembled quantum dots, J. Lumin. **122-123**, 730 (2007).

[26] R. C. Miller, D. A. Kleinman, A. C. Gossard, and O. Munteanu, Biexcitons in GaAs quantum wells, Phys. Rev. B **25**, 6545 (1982).

[27] Z. Sobiesierski, D. A. Woolf, A. Frova, and R. T. Phillips, Photoluminescence and photoluminescence excitation spectroscopy of H-related defects in strained $In_xGa_{1-x}As$/GaAs(100) quantum wells, J. Vac. Sci. Technol. B **10**, 1975 (1992).

[28] L. Allen and J. H. Eberly, *Optical Resonance and Two-Level Atoms* (Wiley, New York, 1975).

[29] J. Shah, *Ultrafast Spectroscopy of Semiconductors and Semiconductor Nanostructures*, Springer Series in Solid-State Sciences Vol. 115 (Springer, Berlin, 1996).

[30] M. Lindberg, R. Binder, and S. W. Koch, Theory of the semiconductor photon echo, Phys. Rev. A **45**, 1865 (1992).

[31] O. Madelung, W. von der Osten, and U. Rössler, *Intrinsic Properties of Group IV Elements and III-V, II-VI and I-VII Compounds*, edited by O. Madelung (Springer, Berlin, 1987).

[32] M. M. Glazov, *Electron & Nuclear Spin Dynamics in Semiconductor Nanostructures* (Oxford University Press, Oxford, 2018), Vol. 1.

[33] A. P. Heberle, W. W. Rühle, and K. Ploog, Quantum Beats of Electron Larmor Precession in GaAs Wells, Phys. Rev. Lett. **72**, 3887 (1994).

[34] A. Malinowski, D. J. Guerrier, N. J. Traynor, and R. T. Harley, Larmor beats and conduction electron g factors in $In_xGa_{1-x}As$/GaAs quantum wells, Phys. Rev. B **60**, 7728 (1999).

[35] A. Malinowski and R. T. Harley, Anisotropy of the electron g factor in lattice-matched and strained-layer III-V quantum wells, Phys. Rev. B **62**, 2051 (2000).

[36] X. Marie, T. Amand, P. Le Jeune, M. Paillard, P. Renucci, L. E. Golub, V. D. Dymnikov, and E. L. Ivchenko, Hole spin quantum beats in quantum-well structures, Phys. Rev. B **60**, 5811 (1999).

[37] Y. G. Kusrayev, A. V. Koudinov, I. G. Aksyanov, B. P. Zakharchenya, T. Wojtowicz, G. Karczewski, and J. Kossut, Extreme In-Plane Anisotropy of the Heavy-Hole g Factor in (001)-CdTe/CdMnTe Quantum Wells, Phys. Rev. Lett. **82**, 3176 (1999).

[38] S. V. Poltavtsev, I. A. Yugova, A. N. Kosarev, D. R. Yakovlev, G. Karczewski, S. Chusnutdinow, T. Wojtowicz, I. A. Akimov, and M. Bayer, In-plane anisotropy of the hole g factor in CdTe/(Cd,Mg)Te quantum wells studied by spin-dependent photon echoes, Phys. Rev. Research **2**, 023160 (2020).

[39] A. V. Trifonov, I. A. Akimov, L. E. Golub, E. L. Ivchenko, I. A. Yugova, A. N. Kosarev, S. E. Scholz, C. Sgroi, A. Ludwig, A. D. Wieck, D. R. Yakovlev, and M. Bayer, Homogeneous optical anisotropy in an ensemble of InGaAs quantum dots induced by

strong enhancement of the heavy-hole band Landé parameter q, Phys. Rev. B **104**, L161405 (2021).

[40] H. M. Tholen, J. S. Wildmann, A. Rastelli, R. Trotta, C. E. Pryor, E. Zallo, O. G. Schmidt, P. M. Koenraad, and A. Y. Silov, Active tuning of the g-tensor in InGaAs/GaAs quantum dots via strain, Phys. Rev. B **99**, 195305 (2019).

[41] S. Wu, K. Peng, X. Xie, J. Yang, S. Xiao, F. Song, J. Dang, S. Sun, L. Yang, Y. Wang, S. Shi, J. He, Z. Zuo, and X. Xu, Electron and Hole g Tensors of Neutral and Charged Excitons in Single Quantum Dots by High-Resolution Photocurrent Spectroscopy, Phys. Rev. Applied **14**, 014049 (2020).

[42] E. A. Zhukov, V. N. Mantsevich, D. R. Yakovlev, I. S. Krivenko, V. V. Nedelea, D. Kowski, A. Waag, G. Karczewski, T. Wojtowicz, and M. Bayer, Magnetic field dependence of the in-plane hole g factor in ZnSe- and CdTe-based quantum wells, Phys. Rev. B **103**, 125305 (2021).

[43] Y. G. Semenov and S. M. Ryabchenko, Effects of photoluminescence polarization in semiconductor quantum wells subjected to an in-plane magnetic field, Phys. Rev. B **68**, 045322 (2003).

[44] I. A. Yugova, A. Greilich, E. A. Zhukov, D. R. Yakovlev, M. Bayer, D. Reuter, and A. D. Wieck, Exciton fine structure in InGaAsGaAs quantum dots revisited by pump-probe Faraday rotation, Phys. Rev. B **75**, 195325 (2007).

[45] https://rscf.ru/en/project/22-22-00439/.

[46] L. D. Landau and E. M. Lifshitz, *Quantum Mechanics*, 3rd ed. (Pergamon, Oxford, 1977).

[47] *Spin Physics in Semiconductors*, edited by M. I. Dyakonov, Springer Series in Solid-State Sciences Vol. 157 (Springer, Berlin, 2008).

[48] M. Bayer, G. Ortner, O. Stern, A. Kuther, A. A. Gorbunov, A. Forchel, P. Hawrylak, S. Fafard, K. Hinzer, T. L. Reinecke, S. N. Walck, J. P. Reithmaier, F. Klopf, and F. Schäfer, Fine structure of neutral and charged excitons in self-assembled In(Ga)As/(Al)GaAs quantum dots, Phys. Rev. B **65**, 195315 (2002).

[49] G. L. Bir and G. E. Pikus, *Symmetry and Strain-Induced Effects in Semiconductors* (Wiley, New York, 1974).

[50] H. W. van Kesteren, E. C. Cosman, F. J. A. M. Greidanus, P. Dawson, K. J. Moore, and C. T. Foxon, Optically Detected Magnetic Resonance Study of a Type-II GaAs-AlAs Multiple Quantum Well, Phys. Rev. Lett. **61**, 129 (1988).

[51] H. W. van Kesteren, E. C. Cosman, W. A. J. A. van der Poel, and C. T. Foxon, Fine structure of excitons in type-II GaAs/AlAs quantum wells, Phys. Rev. B **41**, 5283 (1990).

[52] M. O. Scully and M. S. Zubairy, *Quantum Optics* (Cambridge University Press, Cambridge, 1997).